On Computing the Thermal Flux in Ex-Core Neutron Activation Studies

(Project No. 05-08453)

Dr. John R. White

Chemical and Nuclear Engineering Department

University of Massachusetts Lowell

January 20, 2000

On Computing the Thermal Flux in Ex-Core Neutron Activation Studies

Dr. John R. White
Chemical and Nuclear Engineering Department
University of Massachusetts Lowell

January 20, 2000

Overview

Neutron activation analyses usually require two major areas of effort. One first tries to accurately compute the space-energy neutron flux distribution throughout the geometry of interest. Then, with a known neutron environment, the activation calculations can be performed with a tool such as ORIGENS[1] or ACTIV.[2-3] This second part of the computations is extremely important, and the available codes offer individual advantages and disadvantages. However, the quality of any activation calculation is directly tied to the accuracy of the neutron transport methodology used to determine the space-energy neutron flux in the ex-core regions of the system.

One common method for determining ex-core flux distributions involves coupling DORT 2-D transport computations[4] with use of the BUGLE-96 cross section library.[5] The DORT/ BUGLE-96 combination has been used extensively in pressure vessel fluence studies,[6] and in prior activation analysis benchmarks with the ACTIV code.[3] The BUGLE-96 library was collapsed from the VITAMIN-B6 fine-group library[7] with specific focus on shielding applications. The BUGLE-96 coupled neutron-gamma library has become a standard for many radiation transport applications because it contains the latest ENDF/B-VI data, it already has a well-established user base, and it is readily available to the general user community. However, it is not usually considered as a database of choice for determining thermal neutron fluxes and reaction rates, since the energy resolution at low energy is rather poor (only two energy groups below 0.4 eV).

For activation analyses, in particular, one requires knowledge of the full energy spectrum, including adequate resolution at fast, intermediate, and thermal energies. The fast and epithermal resolution is necessary to get accurate transport of the particle flux from the core source region to the ex-core structural components -- which can be several meters away from the actual fueled core region. And, at these ex-core activation locations, knowledge of the thermal neutron flux magnitude and spectrum is important for accurate computation of the thermal activation rates. The BUGLE-96 47-group neutron cross sections certainly satisfy the energy resolution criteria above thermal, with 18 groups above 1 MeV, 26 groups above 0.1 MeV, and 42 groups above 5 eV. However, with only 5 groups below 5 eV and only 2 groups below 0.4 eV, the thermal range -- which is probably the most important energy region for activation analyses -- may not have sufficient resolution for accurate determination of the thermal flux and thermal activation rates.

Thus, the purpose of this study was to evaluate the required thermal energy resolution needed for accurate ex-core activation analyses. Since the BUGLE-96 library represents a standard for high and intermediate neutron transport, we decided to generate a library similar to

BUGLE-96 that contains additional thermal energy groups. This approach would highlight just the differences due to the thermal energy structure -- allowing one to focus only on the question at hand.

The approach taken to complete the study was broken into three main tasks:

1. Develop and test a procedure for generating new thermally-enhanced datasets that have identical structure to the BUGLE-96 library -- except for the additional thermal energy groups.
2. Using the 199-group VITAMIN-B6 library as the "truth", numerically evaluate the performance of various broad-group approximations. The goal here was to determine the thermal resolution needed to give broad-group and fine-group results that agree to within $\pm 10\%$.

   Note: Since upscatter becomes important in libraries with multiple thermal energy groups, we also needed to evaluate the issues associated with the upscatter versus no-upscatter option that is available when generating the broad-group transport library. In addition, the use of the full upscatter treatment within the DORT transport computation requires that multiple outer iterations be used to converge the thermal fluxes. Thus, this capability also needed to be tested and evaluated.
3. Finally, once a new library has been generated, its performance needs to be fully evaluated -- preferably against measured activation data if possible. For this part of the study, we used the 2-D RZ JPDR model[8] to give a final measure of the performance of the new thermally-enhanced libraries. Previous activation benchmark results using an ACTIV/DORT/BUGLE-96 combination were available,[3] and these data were regenerated using identical models and methods, except for the substitution of a new library to do the transport calculations.

The details and results of the study outlined above are documented in the remainder of this report. The report first establishes our ability to generate BUGLE-like libraries with additional thermal resolution. It then evaluates the performance of several libraries, with and without upscatter, relative to the base 199-group VITAMIN-B6 library for a generic 1-D PWR model[5] and a 1-D radial model of the Japan Power Demonstration Reactor (JPDR).[8] Finally, it summarizes the activation analysis results for the 2-D JPDR benchmark with selected libraries. The report concludes with summary conclusions and recommendations that suggest that a generic BUGLE-like library with multiple thermal groups could significantly increase the range of applicability of the library. In particular, such a library could enhance our ability to perform ex-core neutron activation computations with increased confidence and greater accuracy. If high accuracy is needed, a BUGLE-like library with additional thermal groups coupled with a 2-D DORT computation is recommended as the best available methodology to evaluate the needed thermal fluxes and reaction rates. Although the additional thermal groups with full upscatter capability results in a larger computational burden, the benefits of improved accuracy and reduced uncertainty seem to be well worth the additional effort.

New Library Generation

The methodology for generating new BUGLE-like cross section libraries followed the exact procedures as documented in the BUGLE-96 report.[5] A brief overview is given here to summarize the overall process. The reader is referred to Ref. 5 for further details, as needed.

The goal here is to develop a pseudo problem-independent library that can be utilized for generic neutron transport applications in LWR systems -- including the capability to estimate, with reasonable accuracy, the thermal flux in structures some distance from the original particle source. The starting point is the VITAMIN-B6 fine-group ENDF/B-VI library with 199 neutron groups and 42 gamma groups. Five sets of self-shielded cross sections were generated for a generic PWR cell, a BWR cell, a water-iron mixture, concrete, and typical steel compositions. Several modules of the SCALE 4.3 system,[1] including AJAX, BONAMI, and NITAWL, were used to extract the proper isotopes, do the resonance shielding, and combine the data into a single working library.

The fine-group working library from the first phase of calculations was then used within a 1-D XSDRN[1] model of a typical BWR system and a 1-D XSDRN representation of a generic PWR core with surrounding structures. Spectra from a specific location in the BWR core, PWR core, PWR downcomer, PWR pressure vessel (1/4 thickness), and PWR concrete regions were selected as representative weight functions to collapse the fine-group library into the broad-group structure of interest. The fine-group spectra, obtained from the 1-D BWR and 1-D PWR XSDRN calculations, were only computed once. The various broad-group libraries all used the same weight functions -- only the collapsed broad-group structures were different. Since this study only addressed variations in the thermal region, the < 5 eV region was the only energy structure that was changed for each case. Also, since we were not interested in gamma transport, this component of the dataset was eliminated completely as part of the processing.

The actual collapse from 199 neutron groups to some subsequent level was done with the MALOCS module that is distributed as part of the SCALE 4.3 system. MALOCS collapses the original data with a user-defined weight function (as discussed above). Six actual runs were made that match a particular set of self-shielded isotopes with a particular weight function. As a final step, the six individual collapsed libraries are combined into a single working library for subsequent use in broad-group 1-D XSDRN calculations, and into a single ANISN-formatted library for subsequent 2-D DORT analyses.

The MALOCS step also gives the user an option to create a collapsed library with no upscatter. The BUGLE-96 library used in most shielding applications and in the prior JPDR activation benchmark had the upscatter truncation switch selected within MALOCS. This option makes a rather crude approximation (see further details in the MALOCS input guide in Ref. 1), but it is often adequate if there are only a few broad thermal groups or if the application of interest is not overly sensitive to the thermal flux. In addition, if there is no upscatter present, then fixed-source problems in the DORT and XSDRN transport codes only require a single outer iteration for convergence of the group fluxes -- and this leads to significant reductions in runtime, especially for the 2-D calculations. Thus, if appropriate, the no-upscatter option does offer some benefit. However, it is important to emphasize that for activation analysis computations, accurate knowledge of the thermal flux is essential and the no-upscatter option is probably not appropriate except for the special case of only a few thermal groups.

Following the above outline, several new BUGLE-like datasets were generated, including two 47-group libraries with and without upscatter, two 52-group libraries with and without upscatter, and a single 58-group library with full upscatter. Obviously, the 52-group and 58-group libraries were developed for evaluating the sensitivity of the thermal fluxes and thermal activation calculations to the number of thermal groups relative to the base 47-group BUGLE-96 library. The with-upscatter and without-upscatter libraries were generated to test the importance of the full upscatter treatment as the number of thermal groups was increased. Finally, the base 47-group library with no upscatter was generated as a test of the overall library-generation procedure. This library was expected to be nearly identical to the base BUGLE-96 library, since the same procedures -- taken directly from Ref. 5 -- were used. Also, since the number of isotopes and the isotope order are identical, the new library can be used as a direct replacement for BUGLE-96 in prior DORT calculations. Thus, once the libraries are available, their use in prior DORT studies is a relatively simple process.

As an initial test of the library-generation process, the reference JPDR RZ model used in previous activation analysis benchmark calculations[3] was used with the new 47-group library with no upscatter (which is consistent with the BUGLE-96 dataset used in the earlier calculations). A wire-mesh zone map showing the key material boundaries in the JPDR model is given in Fig. 1 (further details of the models are given in Refs. 3 and 8). The reason for choosing the JPDR model for testing is that several experimental measurements of specific activity were made at various locations in the JPDR. Three areas of particular interest include several radial points in the pressure vessel (PV) along the 360 cm line, five axial locations along the inside of the PV liner, and three experimental locations along the core shroud. These locations are highlighted in the JPDR zone map in Fig. 1.

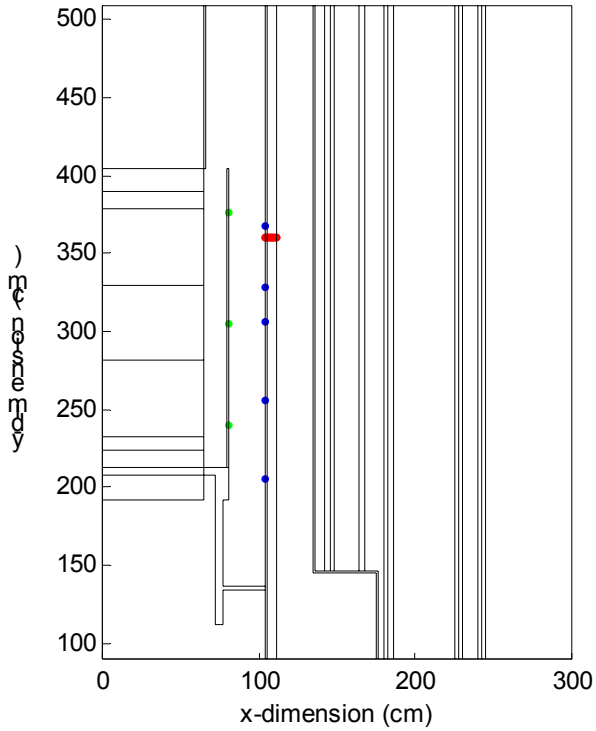

Fig. 1 JPDR zone map with selected measurement points.

For easy comparison of the DORT results, the 47-group fluxes were collapsed to three groups, where the fast flux (group 1) includes energies above 0.1 MeV, the thermal flux range (group 3) includes energies below 0.4 eV, and group 2, the epithermal group, represents all energies between the thermal and fast cutoffs. Also, for easy comparison, most of the results are presented as ratio plots, where perfect agreement gives a straight line at the 1.0 level, and any deviation from the reference case appears as variations above or below unity.

For the current comparisons, we have chosen to present results in terms of full radial profiles at 360 cm and axial profiles at the PV liner. These profiles are displayed in Figs. 2 and 3, respectively. These flux ratio curves compare the broad-group fluxes from the 2-D JPDR model using the new 47-group no-upscatter library versus the BUGLE-96 library (with no upscatter). As apparent, the fast and epithermal fluxes agree almost exactly, but the thermal fluxes are roughly 10-20% higher in many locations for the new 47-group library. This result was not expected, since the library generation process was taken directly from Ref. 5. Obviously, some differences in the inputs or the actual codes used must be causing the observed variations. After nearly exhaustive error checking, an explicit cause of these differences could not be identified. However, we feel that the new library represents the better of the two libraries (new 47-group library versus BUGLE-96). This conclusion is justified since a newer version of XSDRN and a very tight convergence check were used in the current development.[9] Sensitivity studies with XSDRN also show that a loosely converged thermal flux could easily give the differences observed here. Even with the observed variations in thermal flux, we feel that the basic procedure for the generation of the new BUGLE-like libraries has been validated (at least to the extent possible at this time). Thus, these libraries can be used as needed in subsequent analyses.

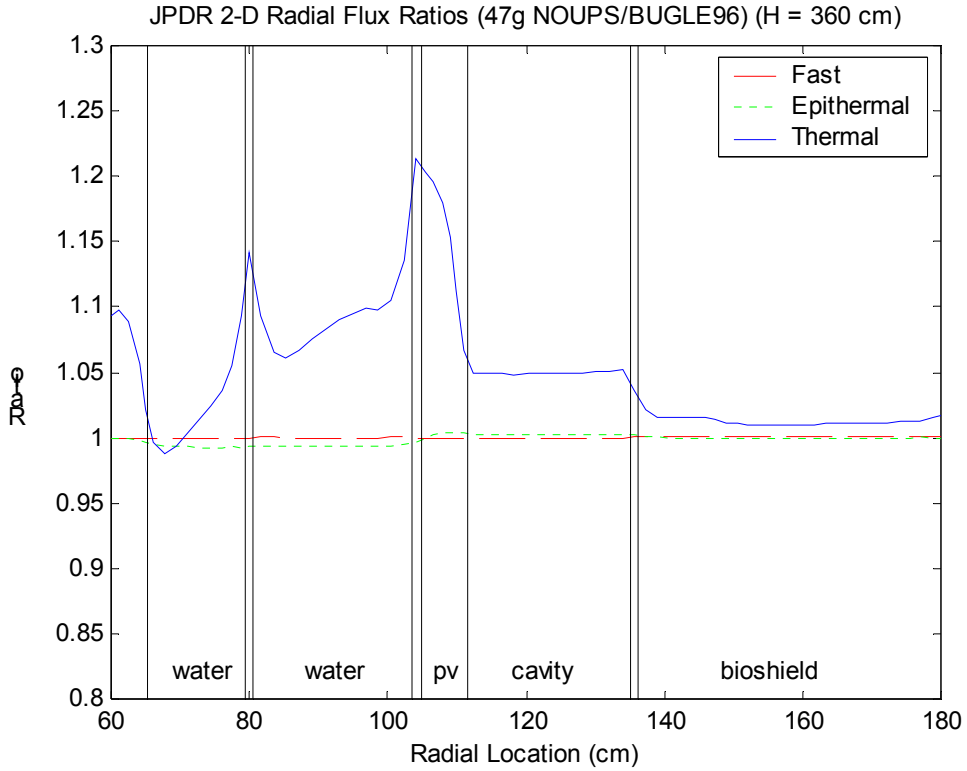

Fig. 2 Radial flux ratios at 360 cm for the 47g no-upscatter library relative to BUGLE-96.

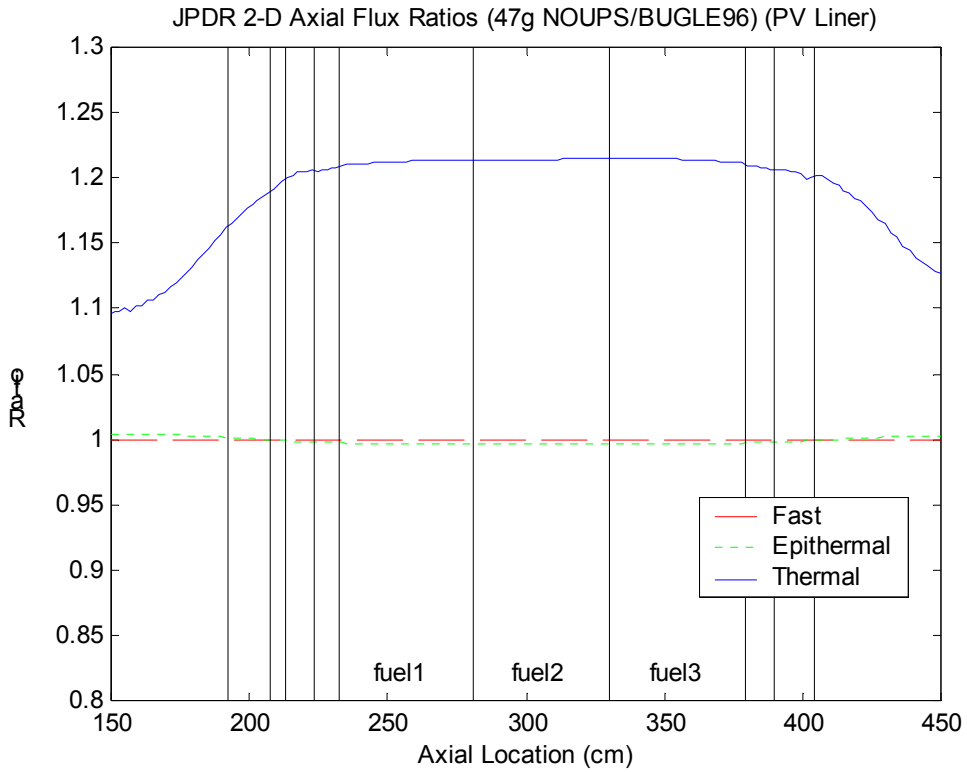

Fig. 3 Axial flux ratios at PV liner for the 47g no-upscatter library relative to BUGLE-96.

Sensitivity to the Thermal Resolution and to the Upscatter Treatment

The original goal of this study was to address the importance of the energy group structure for the thermal energy range within the transport cross section library. Three libraries containing 47, 52, and 58 groups were developed to address this subject. However, all three libraries have identical group boundaries for groups 1-42 and these are the same as the standard BUGLE-96 group structure. Clearly, of importance here is the energy structure below 5 eV, and this information is summarized in Table I for all three libraries. Thus, as seen in Table I, the libraries to be compared include 5, 10, and 16 thermal groups.

Also of note is the number of energy groups below about 0.4 eV, since this is the cutoff used to define the integral thermal flux. Again, as shown in Table I, the three libraries have 2, 5, and 10 groups, respectively, below 0.4 eV. In subsequent comparisons, the fluxes in these groups are summed to give the "thermal" flux, and the additional thermal contribution between 0.4 eV and 5 eV is added to the "epithermal" flux component (for the 3-group representation used to display the results).

From a computational perspective, DORT fixed-source calculations with upscatter are usually avoided if possible because of the significant additional cost associated with the outer iterations needed to converge the upscatter source. In practice, the 47-group BUGLE-96 library with no upscatter is the standard choice for most applications of this library, although a similar library with upscatter is available.[5] In a similar fashion to Ref. 5, both no-upscatter and with-upscatter libraries were generated for the 47-group and 52-group energy structures. Thus, we

can easily address the importance of the full upscatter treatment and evaluate if the additional computational cost associated with the upscatter iterations is needed and/or justifiable.

Table I Energy boundaries in the thermal range for the 47, 52, and 58 group libraries.

Upper Energy (eV)	47g Library Group Number	52g Library Group Number	58g Library Group Number
5.0435	43	43	43
3.0598			44
1.8554	44	44	45
1.1253		45	46
0.8764	45	46	47
0.6251		47	48
0.4140	46	48	49
0.3250			50
0.2250		49	51
0.1500			52
0.1000	47	50	53
0.0700			54
0.0400		51*	55
0.0210			56
0.0100		52	57
0.0020			58

* The upper boundary for Group 51 in the 52-group set is 0.05 eV.

Two XSDRN 1-D radial core models were used to test the various cross section libraries. The first model used was the generic PWR model from Ref. 5. This was the model used to determine most of the weight functions for collapsing the 199g VITAMIN-B6 library. The 199-group fluxes for this case represent the reference or "exact" answer, and all the other broad-group results were compared to this reference. Since the spectra used to collapse the cross sections were derived from this model, the broad-group results for the same PWR model were expected to show fairly good agreement -- since the basic premise of the collapsing process tries to maintain consistent reaction rates in the fine-group and broad-group cases.

As a more rigorous test of the new libraries, a 1-D radial model of the JPDR system was also developed. This small BWR core model represents a 1-D radial cut along the core centerline of the 2-D RZ JPDR model from Refs. 3 and 8. It is quite different in terms of the material arrangement and region thicknesses from the PWR and BWR models used to collapse the original 199-group library. Thus, it should represent a better evaluation of the new libraries for general use in a variety of LWR shielding applications and activation analysis computations.

Again, a 199-group calculation gave the "exact" result and all the subsequent broad-group JPDR 1-D computations were evaluated relative to this reference.

For presentation purposes, the "exact" 199-group flux profiles were collapsed into the same 3-group structure (fast, epithermal, and thermal) as discussed above. The resultant broad-group flux profiles for the PWR model are shown in Fig. 4 and similar profiles for the 1-D JPDR model are displayed in Fig. 5. These profiles focus on the ex-core regions of the respective models. The first feature of note is the characteristic attenuation of the neutron flux with distance from the core region. Also apparent are the rapid variations in the thermal flux within the large PV region of each model and the peaks that occur at the several water-metal interfaces. These profiles are specific to the particular models used here, but they are qualitatively similar to what is expected in most PWR or BWR ex-core configurations. These reference profiles were generated using the base VITAMIN-B6 library and they are used in the remainder of this section as the basis for comparison of the various broad-group libraries that were evaluated as part of this study.

The primary results from the current sensitivity study are summarized in the series of 3-group flux ratio plots given in Figs. 6-10. Each figure contains two plots -- the top plot shows the flux ratios for the PWR model and the bottom plot shows a similar comparison for the 1-D JPDR model. In all cases, the denominators for the flux ratios contain the 199-group solution with full upscatter (i.e. the profiles shown in Figs. 4 and 5).

Figures 6 and 7 look at the 47-group results without and with upscatter, respectively. As apparent, neither case gives very good results. The no-upscatter case in Fig. 6 tends to seriously under-predict the thermal flux and, to a smaller degree, the epithermal flux in many locations. The thermal flux is generally low by 20-40%, and by more than 60% in the vessel region of the PWR model. The resultant flux ratios for the 47-group upscatter cases, as shown in Fig. 7, go in the other direction and tend to over-predict the thermal flux, with errors as large as 50% in the JPDR model. The PWR model for the upscatter case is fairly reasonable, with the thermal flux ratio less than 1.1 for most of the model -- except for the second half of the PV where the errors go to about 20%.

The 52-group results are summarized in Figs. 8 and 9. Figure 8, in particular, clearly indicates that the no-upscatter approximation is simply not appropriate for applications where the thermal flux plays an important role. The thermal flux ratios decreased even further for the 52-group library relative to the 47-group library with no-upscatter. This implies that, as the number of thermal groups is increased, the proper treatment of upscatter is even more important. With this result, there is no sense continuing to perform additional calculations with the no-upscatter option. Thus, the 47-group calculation will be the only no-upscatter case that is discussed in subsequent sections.

The 52-group upscatter cases, on the other hand, show significant improvement relative to the 47-group upscatter cases. This is indicated clearly in Fig. 9, where the errors for the PWR case are generally within $\pm 6\%$, and the flux ratios for the JPDR model are mostly under 1.15. The only exception is for a portion of the PV in the JPDR where the error in the thermal flux increases to about 25%. However, as seen in Fig. 5, the thermal flux is quite small in this area, so a 25% error in the flux would not lead directly to a 25% error in the total activity in this region. Thus, the 52-group library with 9 upscatter groups is quite reasonable, and it gives acceptable overall flux profiles for use in general ex-core activation calculations.

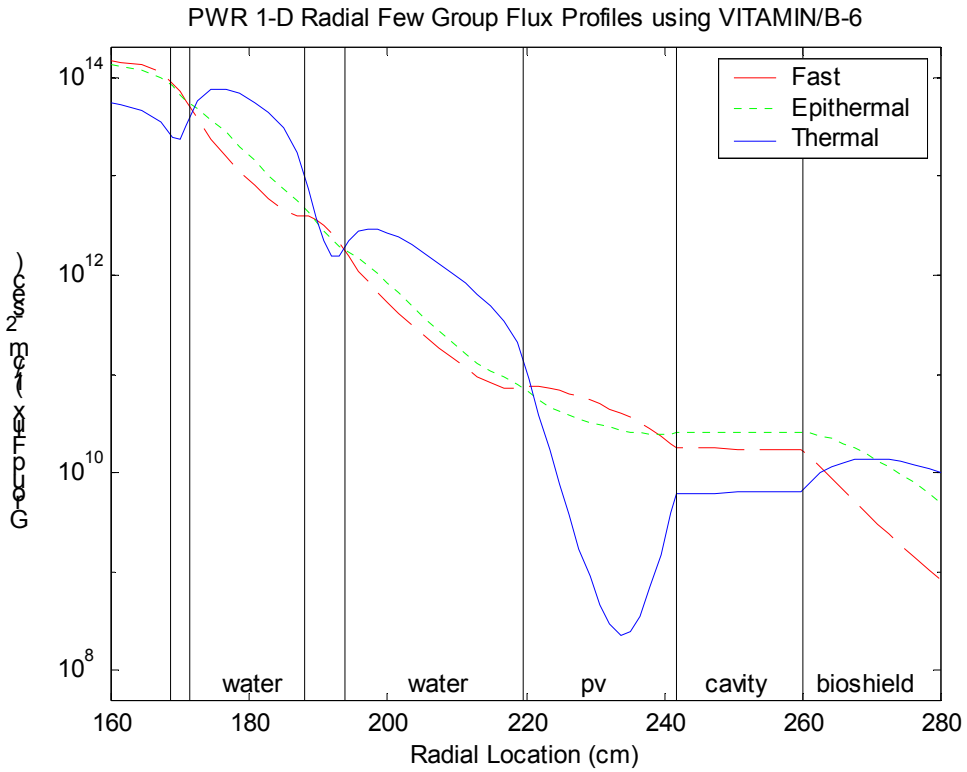

Fig. 4 Reference PWR radial flux profiles (using VITAMIN-B6 library).

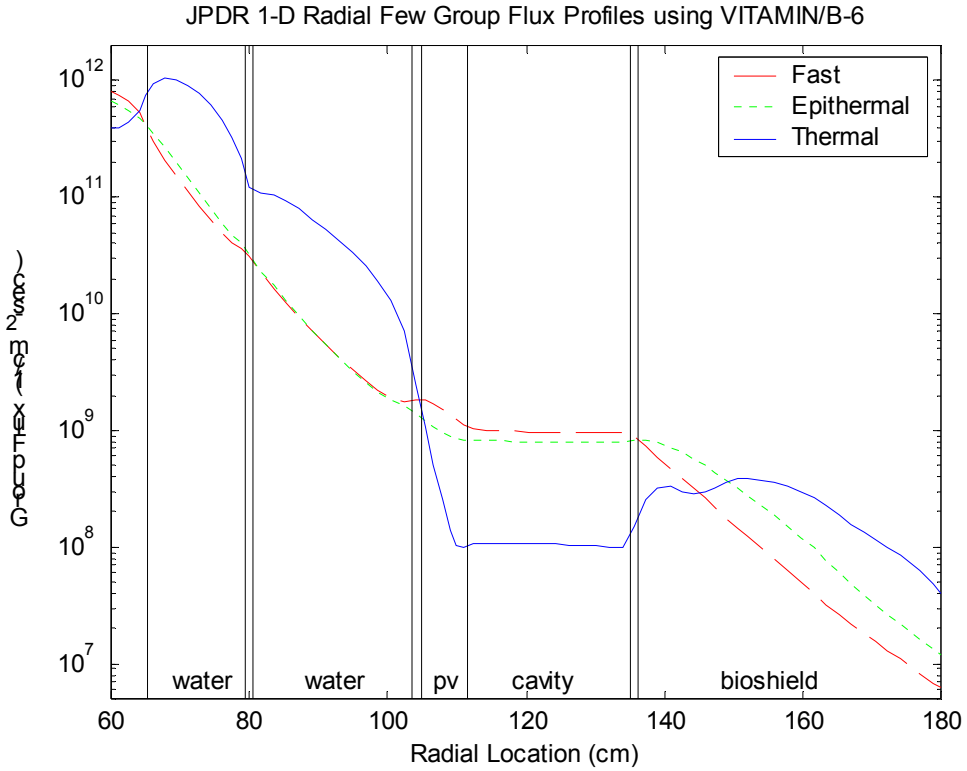

Fig. 5 Reference JPDR radial flux profiles (using VITAMIN-B6 library).

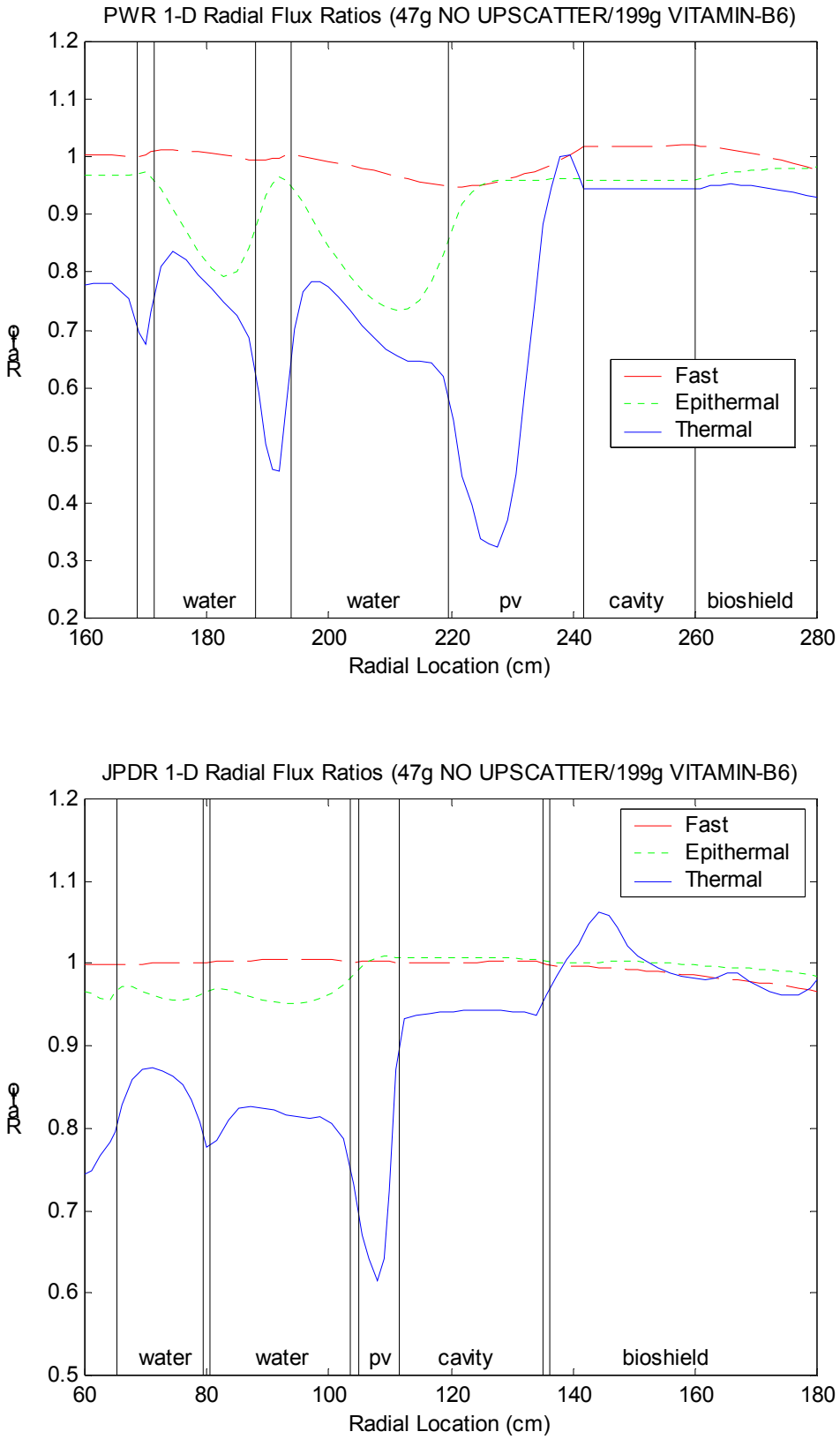

Fig. 6 PWR (top) and JPDR (bottom) flux ratio profiles for the no-upscatter 47g library.

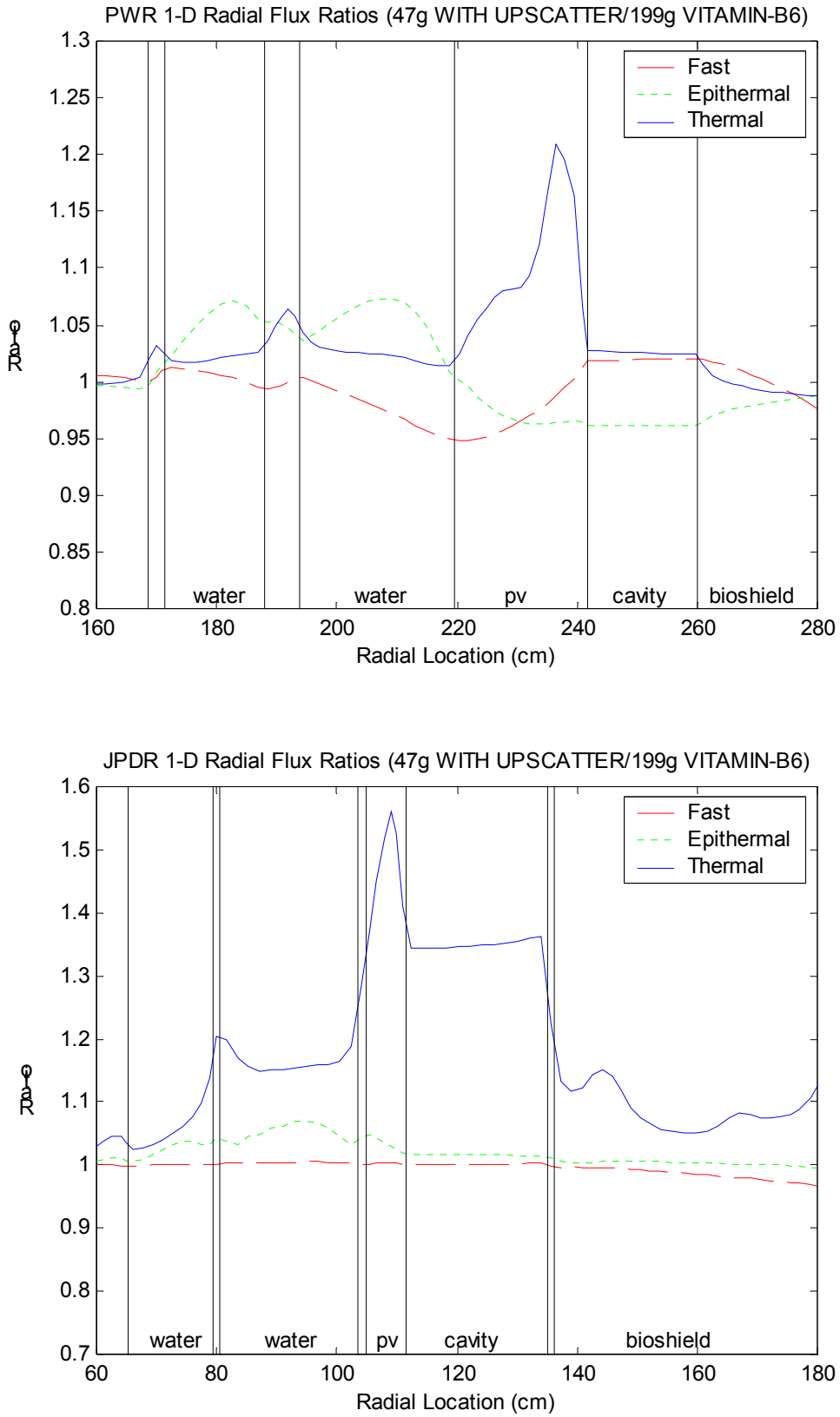

Fig. 7 PWR (top) and JPDR (bottom) flux ratio profiles for the 47g library with upscatter.

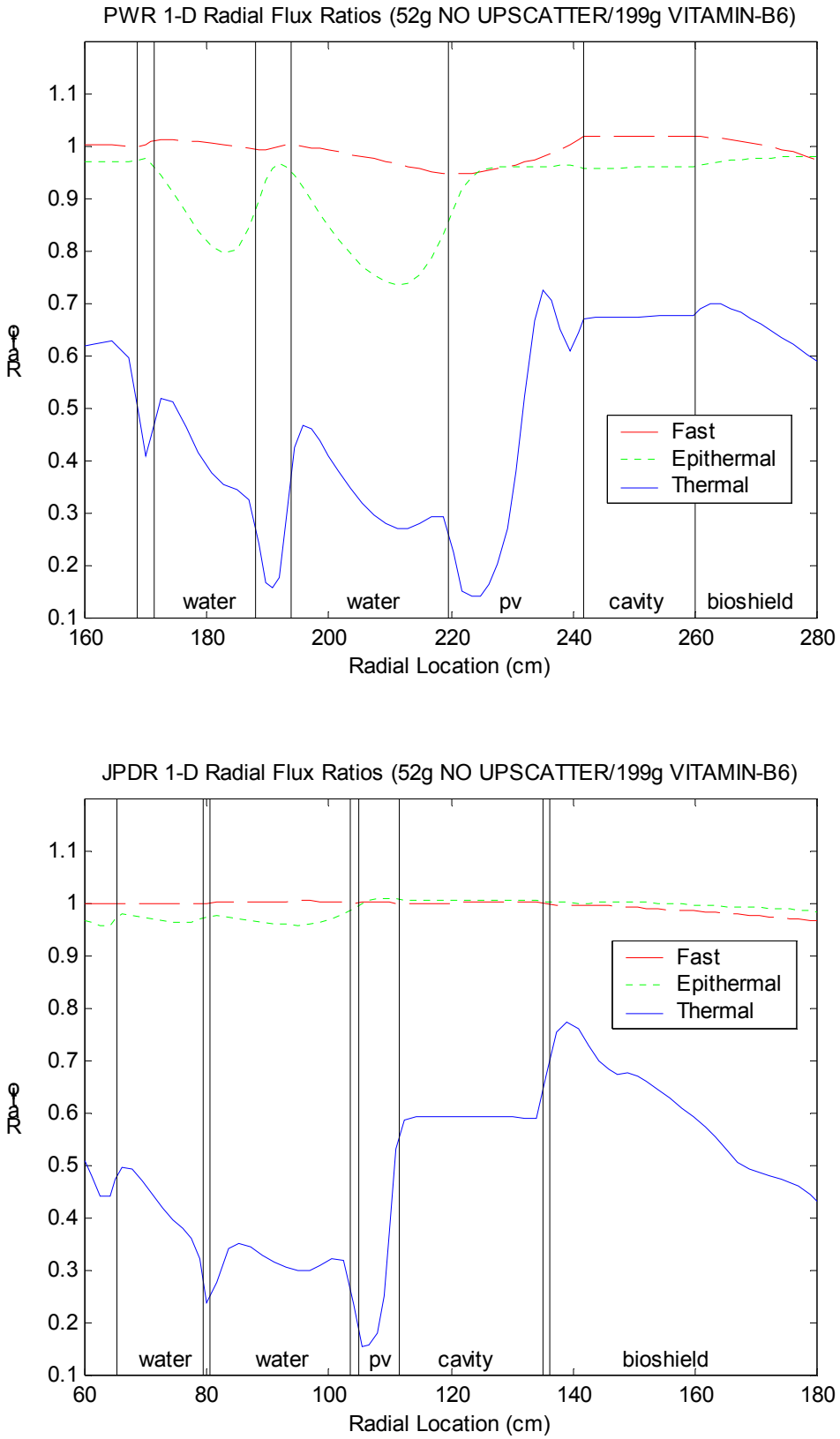

Fig. 8 PWR (top) and JPDR (bottom) flux ratio profiles for the no-upscatter 52g library.

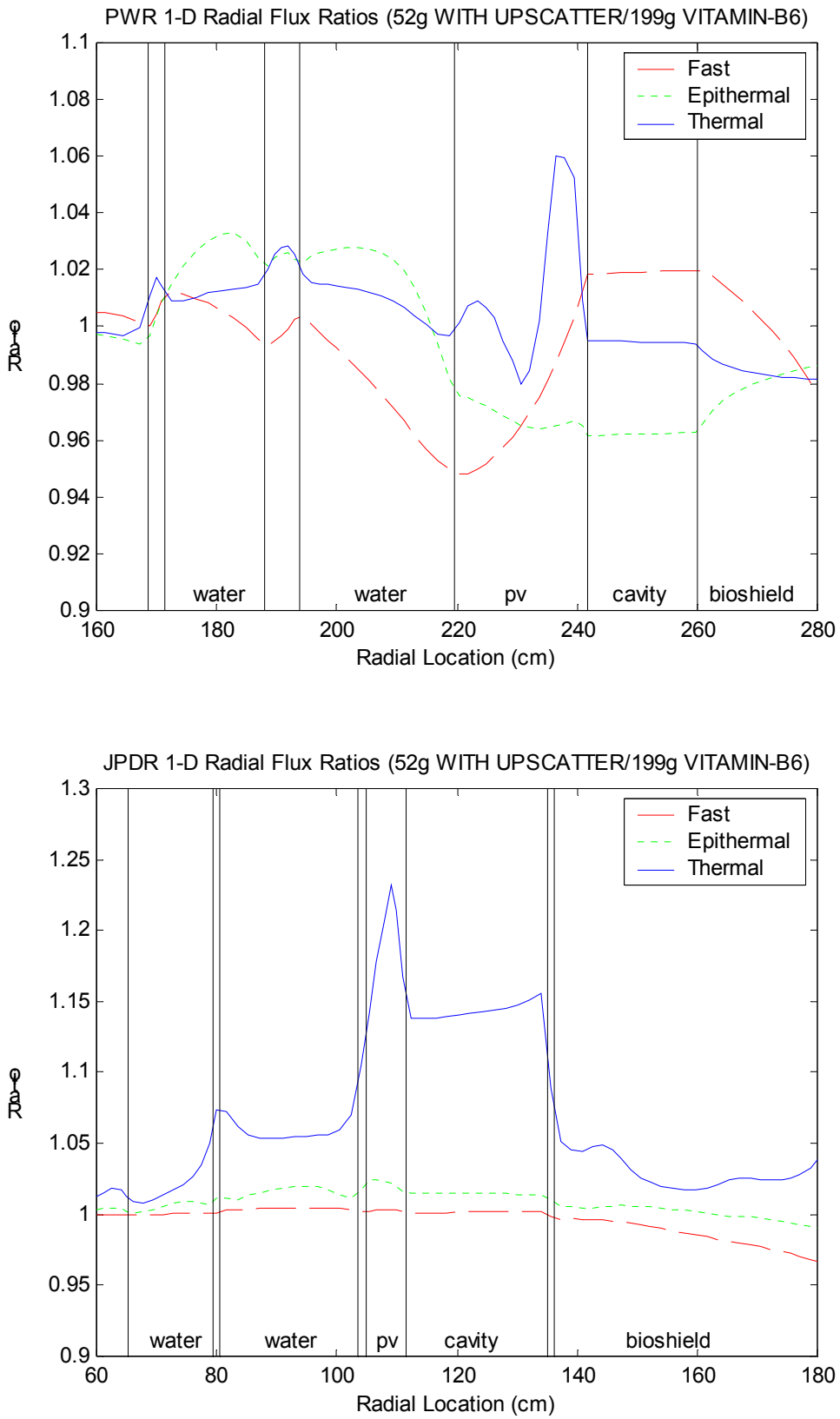

Fig. 9 PWR (top) and JPDR (bottom) flux ratio profiles for the 52g library with upscatter.

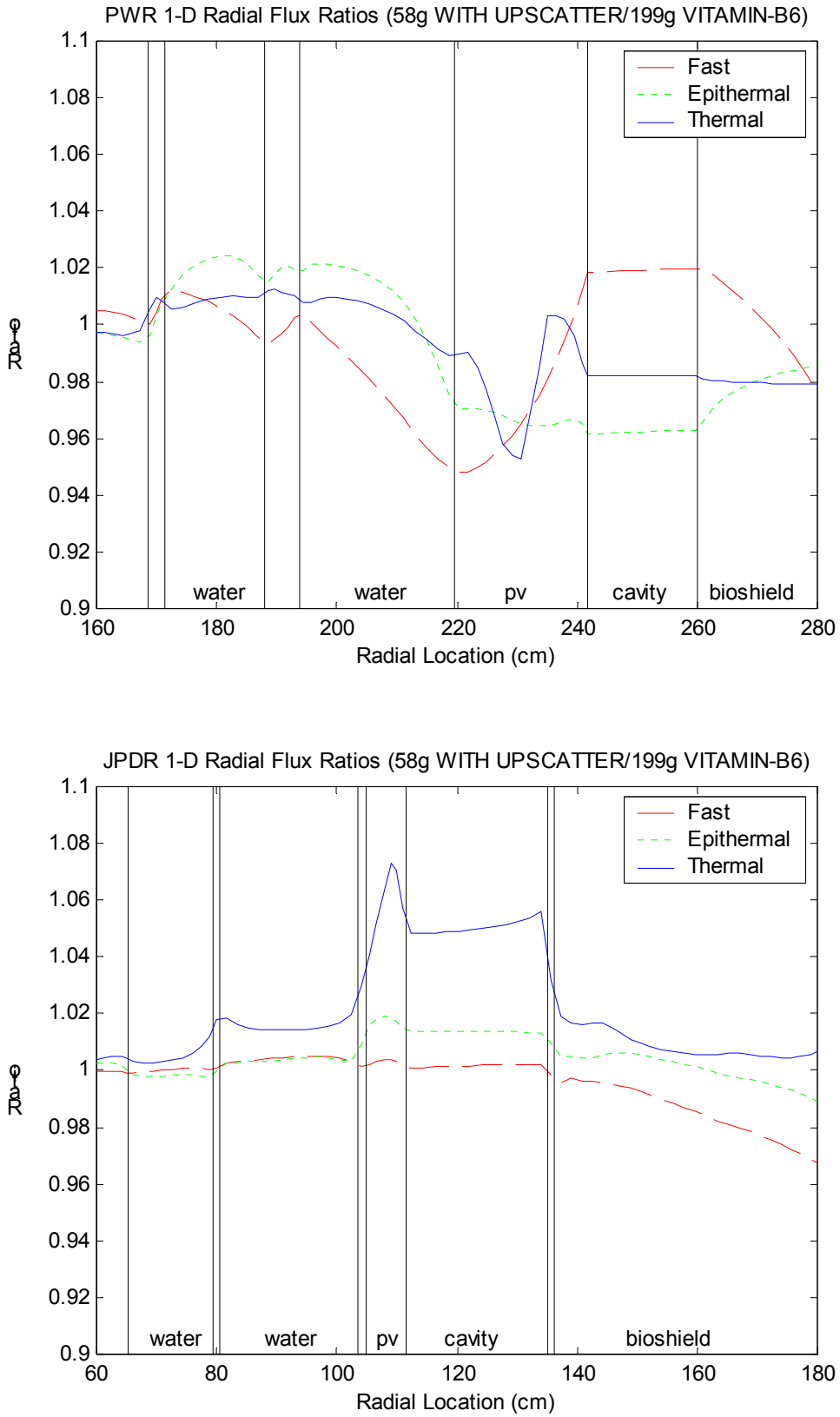

Fig. 10 PWR (top) and JPDR (bottom) flux ratios for the 58g library with upscatter.

Since the error in the JPDR thermal fluxes is still much greater than the error in the PWR model with the 52-group library (see Fig. 9), it is assumed that the sensitivity of the collapsed cross sections to the choice of weight function is still quite high. With the desire for a truly "pseudo problem-independent library" that can be used in a variety of applications, the next step was to try the 58-group library as a means of reducing this spectrum sensitivity. The 58-group library has 10 groups below 0.4 eV, and this should be sufficient resolution for most applications. Also, since the "broad-group" library still contains a lot of energy detail, it should be relatively insensitive to the spectra used in the collapsing step -- and this is exactly what we desire.

The resultant flux ratio profiles from the 58-group tests are summarized in Fig. 10. Here we have finally reached the desired goal of less that 10% error in the fluxes computed with the broad-group library. In fact, the error in the thermal flux in the PWR model is only about $\pm 5\%$ and the uncertainty in the JPDR model is less than 8% in the worse case. These results are quite good, and they say that roughly the same accuracy can be achieved with a 58-group library as that obtained with the original 199-group dataset. Thus, from an accuracy perspective for general applications, the 58-group library with the full upscatter treatment appears to be the best choice of a broad-group library. On the negative side, however, this library has 15 upscatter groups, which will require several outer iterations for convergence of the subsequent DORT transport calculations.

The above analyses can be summarized with the following observations/conclusions:

1. Libraries with low thermal energy resolution tend to over-predict the thermal flux. Recall that the three libraries tested have 5, 10 and 16 thermal groups. The peak over-prediction relative to the 199-group JPDR case, for example, was about 55%, 25%, and 8%, respectively for the three libraries with full upscatter. Thus, more thermal energy groups is definitely better – which is not a surprising result. However, this study has shown that a 16-group structure in the thermal range can give nearly the same accuracy (within $\pm 10\%$) as the 36 thermal groups in the base VITAMIN-B6 library.
2. Using the upscatter truncation option in the MALOCS module produces libraries with no upscatter and these tend to severely under-estimate the thermal flux. In addition, because upscatter is even more important in libraries with a finer group structure, the over-prediction gets worse as the number of thermal groups is increased. Thus, the no-upscatter option is simply not appropriate for libraries with more than 3-5 thermal groups.
3. The over-prediction associated with few thermal groups and the under-prediction related to the no-upscatter option tend to cancel within the 47-group no-upscatter library. This cancellation of errors makes the 47-group no-upscatter library seem reasonable for the JPDR model, with errors on the order of only -20%. This result, however, is somewhat fortuitous, and similar results probably cannot be expected in general analysis (for example, the PWR model under estimates the thermal flux by as much as 60%).
4. The 58-group library with full upscatter is clearly the best of the broad-group libraries studied here. Its performance in general shielding and ex-core activation analysis applications should be roughly similar to the 199-group VITAMIN-B6 library. With its 16 thermal groups, however, several upscatter iterations will be required as part of the transport calculations for accurate prediction of the thermal flux.

Activation Analysis Results for the 2-D JPDR Benchmark

The real test of any new broad-group library is to evaluate its performance relative to experimental measurements for the particular application of interest. In the current study, our focus is on ex-core neutron activation, and the best experimental data available for testing in this area of application are associated with the JPDR activation analysis problem.[8] This problem was put forth as a formal benchmark several years ago by the IAEA[10] and several participants have attempted its solution.[2-3, 11-12] In particular, for this study the computations from Ref. 3 were re-calculated using several of the new libraries discussed in the previous section. The results in Ref. 3 were generated using the 47-group no-upscatter BUGLE-96 library for the transport calculations and a 47-group activation library that was generated directly from VITAMIN-B6 (see Ref. 3 for further details). The present calculations only vary the transport library, leaving the activation library unaltered. For full energy group compatibility, the flux files from the various transport calculations were collapsed to the 47-group level, as needed, before the activation calculations were performed.

Five sets of results are compared here. The BUGLE-96 results from Ref. 3 are considered as reference. The other four computations used the 47-group libraries with and without upscatter, and the 52-group and 58-group libraries with the full upscatter treatment. DORT calculations were performed with each of these datasets and the resultant scalar fluxes were used to do the activation calculations in the ACTIV code.

Four sets of ratio plots are presented in Fig. 11 to highlight the differences in the four new libraries relative to BUGLE-96. The data presented compare the radial flux profiles along an axial cut at 360 cm and they illustrate the differences that one can expect to see in the subsequent activation results. Clearly, any high-energy threshold reactions will not change because the fast flux is essentially identical in all the models. A similar statement is essentially true for reactions that are dominated by the epithermal flux. The thermal flux, on the other hand, is generally larger with all the new datasets relative to the base BUGLE-96 library. This increase, by a factor of 2.5 within the PV in some cases, will definitely increase the thermal activation rates and the subsequent specific activities computed throughout the JPDR model.

The ACTIV code was run with each of the new libraries and summary results from each case are compared directly to the experimental data from JPDR.[8] Here we focus on a subset of the data -- namely the radial activity profiles measured in the PV at H = 360 cm as well as three axial locations in the core shroud and five axial positions along the inner surface of the PV liner. These same locations were highlighted in Ref. 3 (which used the BUGLE-96 library for the DORT flux calculations).

The comparisons for the radial profiles in the PV are displayed in Fig. 12 as calculated-to-experimental (C/E) ratios for all five cases. The top plot has the BUGLE-96 results from Ref. 3 and the other four plots summarize the new results for the two 47-group libraries without and with upscatter and for the 52-group and 58-group datasets with full upscatter. The asterisks in each plot show the actual C/E value at each measurement point and the solid line represents a quadratic fit to these individual points. The fits simply show the general trend in the C/E data. All the C/E values are reasonable, covering a range from about 0.7 to 1.1 at the extremes. The BUGLE-96 C/E values are the lowest and, as implied by the flux ratio plots in Fig. 11, this is consistent with expectations -- since the thermal flux is larger with all the new libraries.

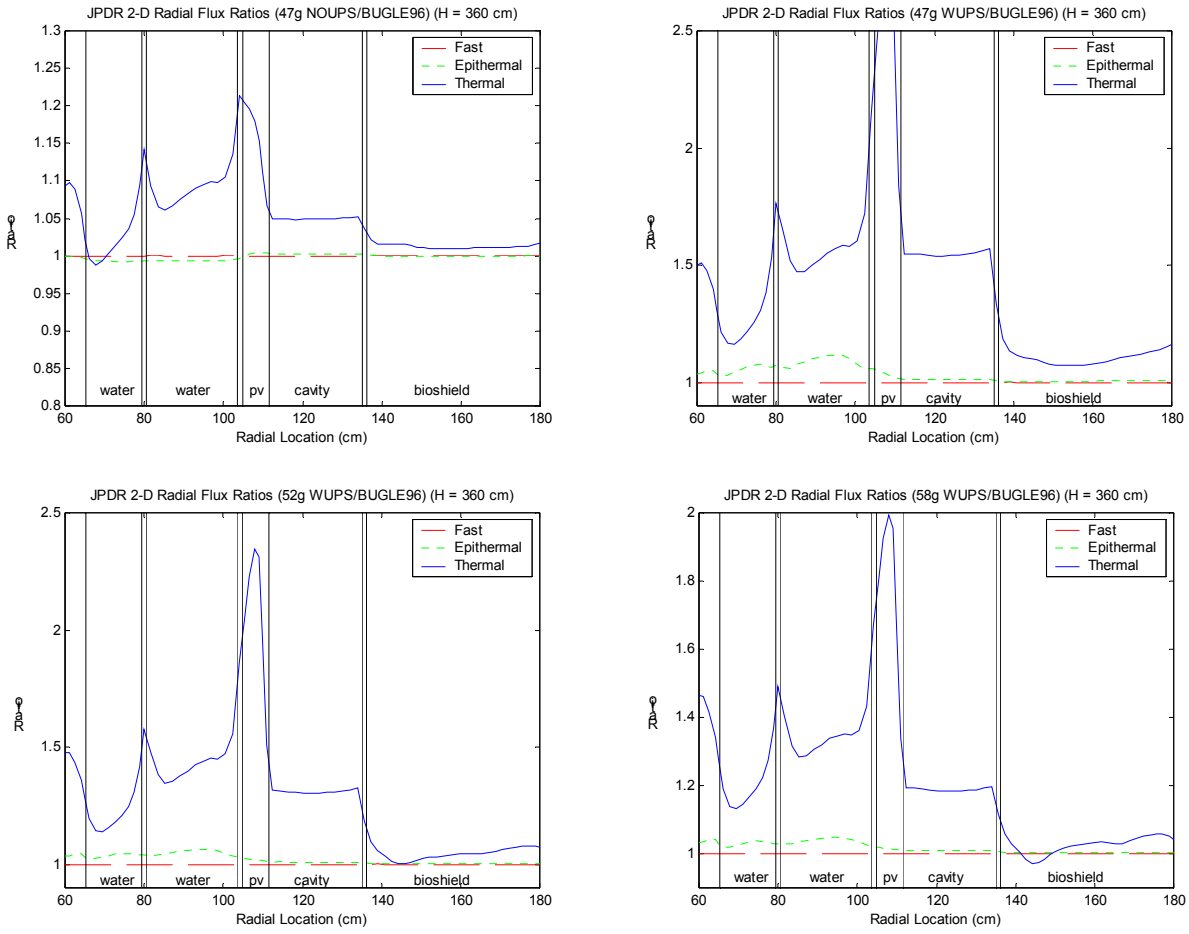

Fig. 11 Radial flux ratio plots at H = 360 cm for four new datasets relative to BUGLE-96.

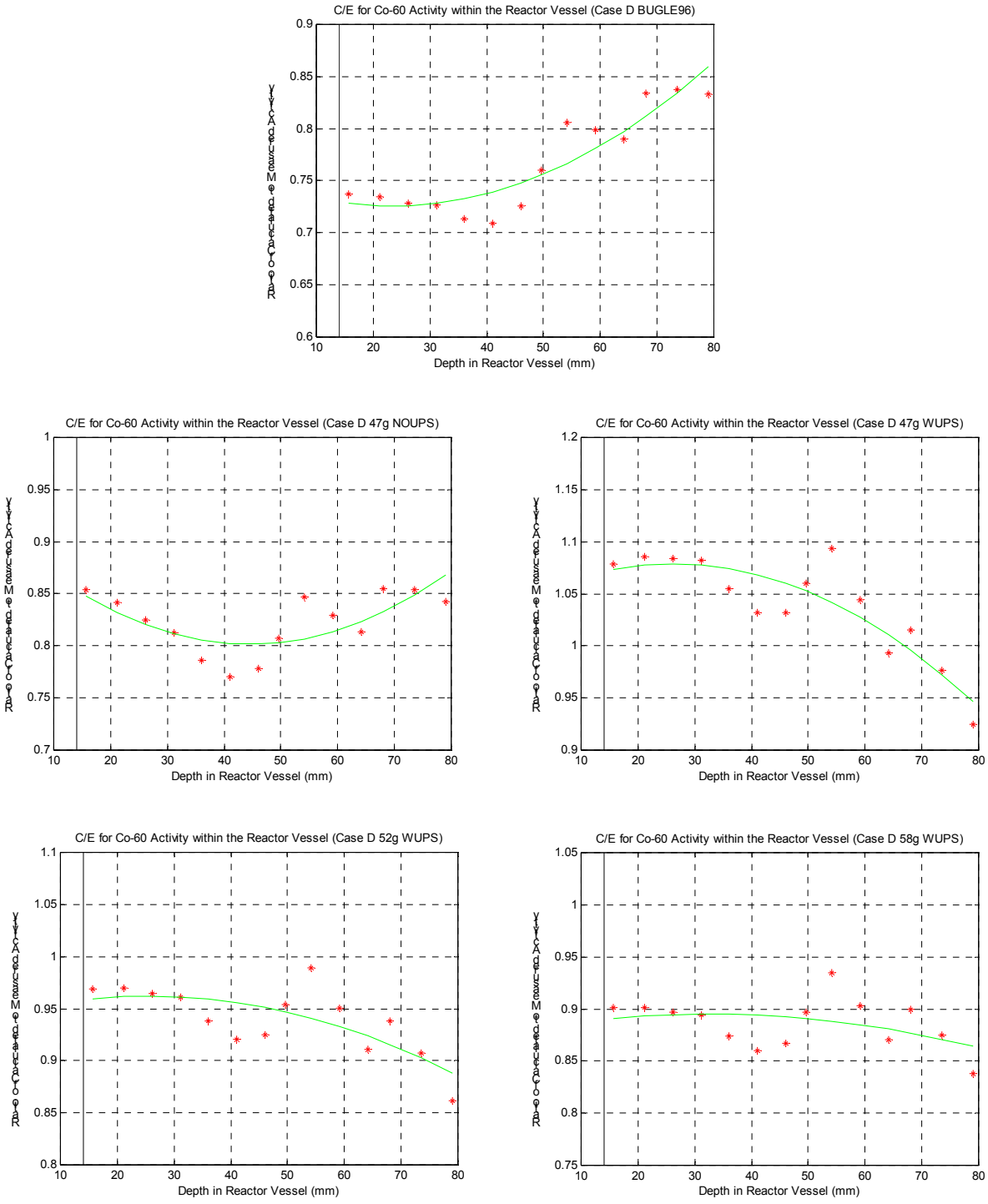

Fig. 12 Radial C/E profiles for the ^{60}Co activity within the reactor vessel.

Note that the y-axis scale in Fig. 12 varies in each plot, but in all cases, it spans a 0.3 range of C/E values. This scale consistency facilitates a comparison of the C/E trend with distance into the vessel. In particular, the three 47-group libraries all show a definite trend in the C/E with distance into the vessel. This implies that the rapidly changing spectrum in the vessel is not well represented with these datasets. The 52-group and 58-group libraries, however, with their increased thermal resolution, do a much better job overall. In fact, the 58-group library shows little or no trend, with a relatively constant C/E of about 0.89 throughout the vessel. This clearly shows the utility of the increased thermal resolution in the 58-group library. Apparently, a significant number of thermal groups is needed to accurately model the large spectral gradients in the JPDR vessel region. This observation may be even more important in activation calculations in PWRs, where the vessel is even larger than in BWRs (recall that the JPDR was a small BWR system and its vessel was only about 7 cm thick).

The C/E data obtained for the axial activity measurements along the core shroud and along the inner side of the PV liner are summarized in Tables II and III, respectively. With only 3 points for the shroud and 5 points for the PV liner, tabulated C/E data seemed more meaningful that plotting the axial profiles. However, there are many numbers in these two tables, and it is not easy to make definitive conclusions regarding the relative merit of different data sets. Clearly, the ^{54}Mn activity data are common for all five libraries because the n,p reaction in ^{54}Fe is a fast threshold reaction and it does not change for the different libraries (that differ only in the thermal region). The remaining activities for ^{55}Fe, ^{60}Co, and ^{63}Ni are dominated by thermal and epithermal neutron capture, and the four new libraries all tend to have larger C/E values relative to BUGLE-96, primarily due to the increase in the thermal flux computed with these transport libraries. These general results are definitely consistent with the radial results shown in Fig. 12 and with previous comparisons of the computed fluxes with the different libraries.

In general, all the libraries tend to over-predict the ^{55}Fe, ^{60}Co, and ^{63}Ni activities along the core shroud. This same statement is true for the lowest point in the PV liner. The C/Es for the remaining four points along the PV liner vary above and below unity, with BUGLE-96 giving generally low values, the 47-group library with upscatter giving a generally high prediction, and the 58-group library showing values that vary in a tight range quite close to unity. In general, however, most of the thermally-dominated C/E values are quite reasonable, and they show general agreement with experiment to within roughly $\pm 30\%$ (most C/E values range from 0.70 to 1.30). There are a few exceptions to this observation, but it appears that $\pm 30-40\%$ error is not an unreasonable expectation in these regions of the model.

In an attempt to summarize the above comparisons, an average C/E and the standard deviation around this mean value were computed for each library and separate set of activities. In particular, Table IV tabulates these results for the radial ^{60}Co activities in the PV and for the axial ^{55}Fe, ^{60}Co, and ^{63}Ni activities along the core shroud and PV liner. These data reinforce the general statements made above but, by themselves, they are not as definitive as hoped. However, noting the superiority of the 58-group library from our previous conclusion concerning each library's ability to accurately represent the thermal flux (from fundamental principles), we also emphasize that the 58-group dataset with full upscatter does a very good job with the JPDR benchmark.

Table II. C/E values at several axial points along the core shroud.

		Point 1	**Point 2**	**Point 3**
	z location (cm)	240	305	376
BUGLE-96 (47g)	^{54}Mn	1.51	0.85	0.99
	^{55}Fe	1.10	0.79	1.20
	^{60}Co	1.03	0.93	1.11
	^{63}Ni	1.18	1.01	1.03
47g No Upscatter	^{54}Mn	1.51	0.85	0.99
	^{55}Fe	1.25	0.90	1.37
	^{60}Co	1.16	1.05	1.25
	^{63}Ni	1.34	1.15	1.17
47g With Upscatter	^{54}Mn	1.51	0.85	0.99
	^{55}Fe	1.38	0.98	1.52
	^{60}Co	1.28	1.15	1.39
	^{63}Ni	1.49	1.27	1.30
52g With Upscatter	^{54}Mn	1.51	0.85	0.99
	^{55}Fe	1.27	0.91	1.39
	^{60}Co	1.18	1.06	1.27
	^{63}Ni	1.36	1.16	1.19
58g With Upscatter	^{54}Mn	1.51	0.85	0.99
	^{55}Fe	1.23	0.88	1.34
	^{60}Co	1.14	1.03	1.23
	^{63}Ni	1.32	1.13	1.15

Table III. C/E values at several axial points along the reactor vessel liner.

		Point 1	**Point 2**	**Point 3**	**Point 4**	**Point 5**
	z location (cm)	206	256	306	328	368
BUGLE-96 (47g)	^{54}Mn	1.91	1.09	1.29	1.18	1.31
	^{55}Fe	1.16	0.74	0.88	0.86	0.90
	^{60}Co	1.13	0.70	0.83	0.81	0.84
	^{63}Ni	1.07	0.69	0.82	0.80	0.84
47g No Upscatter	^{54}Mn	1.91	1.09	1.29	1.18	1.31
	^{55}Fe	1.36	0.89	1.06	1.03	1.08
	^{60}Co	1.30	0.82	0.98	0.95	0.99
	^{63}Ni	1.26	0.83	0.99	0.97	1.01
47g With Upscatter	^{54}Mn	1.91	1.09	1.29	1.18	1.31
	^{55}Fe	1.54	1.08	1.29	1.26	1.31
	^{60}Co	1.45	0.99	1.17	1.15	1.19
	^{63}Ni	1.43	1.02	1.21	1.19	1.23
52g With Upscatter	^{54}Mn	1.91	1.09	1.29	1.18	1.31
	^{55}Fe	1.41	0.97	1.16	1.13	1.18
	^{60}Co	1.34	0.90	1.06	1.04	1.08
	^{63}Ni	1.31	0.91	1.09	1.06	1.10
58g With Upscatter	^{54}Mn	1.91	1.09	1.29	1.18	1.31
	^{55}Fe	1.32	0.90	1.07	1.05	1.09
	^{60}Co	1.27	0.83	0.99	0.97	1.01
	^{63}Ni	1.23	0.84	1.01	0.98	1.02

Table IV Average C/E data and standard deviations for the different libraries.

	Radial ^{60}Co activities in PV		Axial ^{55}Fe, ^{60}Co, and ^{63}Ni activities along shroud		Axial ^{55}Fe, ^{60}Co, and ^{63}Ni activities along PV liner	
Library	Average C/E	Standard Deviation	Average C/E	Standard Deviation	Average C/E	Standard Deviation
BUGLE-96	0.77	0.05	1.04	0.13	0.87	0.14
47g No Upscatter	0.82	0.03	1.18	0.14	1.03	0.16
47g With Upscatter	1.04	0.05	1.31	0.17	1.23	0.15
52g With Upscatter	0.94	0.03	1.20	0.15	1.12	0.15
58g With Upscatter	0.89	0.02	1.16	0.14	1.04	0.14

Overall, the 58-group library tends to under-predict the radial ^{60}Co activities in the PV by only 10-15% with very low variability and essentially no trend in the data with distance into the vessel (see Fig. 12). Although the standard deviation is roughly the same for all the libraries for the axial activities, the 58-group library has one of the best average C/E ratios in the PV liner and a reasonable average C/E value for the core shroud. Thus, based on these data and our previous comparisons, the 58-group library appears to be the best general-purpose transport library for use in generic activation analysis studies.

A cautionary note, however, is not to read too much into a single benchmark exercise. For example, from the data in Table IV, one might wrongly conclude that the new 47-group upscatter library is just as good as the 58-group library for performing general activation analysis studies -- since all the summary indicators are similar for the two libraries. However, our fundamental study comparing the various broad-group libraries to their fine-group base library, showed that, for the JPDR model, there was a fortuitous cancellation of errors associated with only a few thermal groups and the no-upscatter approximation. In another model, with a different material arrangement and different region thicknesses, this cancellation may or may not occur. Thus, additional benchmark data for a variety of situations would help identify these special cases, and more clearly characterize the libraries for general-purpose use.

With the limited measured information available, we placed more emphasis on the basic library characterization study discussed previously when selecting the 58-group library as the best dataset for computing the thermal flux for general activation analysis studies. The JPDR benchmark exercise simply confirms that this library performs quite well for this particular system. Our generic characterization suggests that it probably will also fair well in other situations. Additional benchmark data, however, are needed to prove this hypothesis.

Treating Upscatter Within the DORT Calculations

The last subject to be discussed here considers the actual flux calculation within the DORT code with libraries that include a full upscatter matrix. Most shielding or ex-core activation analysis studies are set up as fixed-source problems. For fixed-source problems with no upscatter (and no fission), DORT only needs to perform a single outer iteration to compute the fluxes in all the energy groups. However, when upscatter is treated, multiple outer iterations are required to converge the thermal fluxes (all the groups that have an inscatter from a lower energy group). Since DORT is primarily used in shielding applications, which often do not put much emphasis on the thermal flux, the upscatter convergence algorithms never received much serious attention. Thus, this part of the calculation is quite slow and often does not converge very well.

To improve efficiency, problems including upscatter are usually broken into two separate calculations. The first part includes only one outer iteration and focuses on converging all the groups above the upscatter cutoff (42 groups in the current calculations). The second part of the computation uses the flux from the first case as a flux guess and it only does additional iterations on the thermal groups. This specification is set in DORT's 28$$ array which sets the number of inner iterations by group. Thus, for the current calculations, setting the first 42 entries in this array to zero bypasses any additional iterations on the non-thermal fluxes from the first phase of the calculation. After multiple outer iterations on just the thermal groups, the output from the second phase of the calculation should have converged fluxes for all energy groups.

The above sequence works nicely in theory, but unfortunately, the second calculation in DORT often converges very slowly or not at all. DORT has upscatter rebalance and fission rescaling to help converge problems with upscatter and/or problems involving fission. For situations with upscatter but no fission, a "trick" suggested several years ago by one of the code authors is sometimes used to help with the upscatter convergence algorithm.[13] This technique first requires that the user replace the $\nu\sigma_f$ cross section is the GIP library with the upscatter cross section. Then, during the calculation, one sets the fission spectrum, χ_g, to a very small value -- effectively removing "fission" from the problem. However, the code thinks that "fission" is still present and it does fission rescaling, with the upscatter scatter cross section instead of the real fission production cross section. Since the upscatter rebalance is also done, DORT effectively applies this rebalance procedure twice. This "trick" often leads to a slightly better convergence rate.

The procedure just outlined was actually used in the current calculations because the normal scheme, without the "fission rescaling trick", simply took too long to converge. An example of the improvement in convergence is illustrated in Fig. 13. This case uses the new 47-group library with full upscatter present. The second part of the calculation was first attempted with only the normal upscatter rebalance scheme (no modifications to the GIP cross sections) with the maximum number of outer iterations set to 30 (ISRMX in the DORT input). This case, as seen in Fig. 13, was only converged to the $3\text{x}10^{-2}$ level and the rate of convergence was so slow that it would easily take 100 or more outers to converge to the desired level of $1\text{x}10^{-3}$. The same case was run again, this time with the modified GIP library with $\nu\sigma_f$ replaced by σ_g^{up}, a very small χ_g, and ISRMX = 40. There was some noticeable improvement after the 12^{th} iteration, but even after 40 outers, the problem was still not converged. A restart case was

completed with another 40 outers and, as seen in Fig. 13, this case could not be converged below about $3x10^{-3}$. Although not overly effective, the "fission rescaling trick" did improve convergence slightly, and this mode of calculation became the procedure used in all the other upscatter cases.

Fig. 13 Effect of the "fission rescaling trick" for the 47-group upscatter case.

Since the level of convergence observed in Fig. 13 was the best that could be obtained in most of the other cases, there was some concern about the accuracy of the "unconverged" DORT-calculated thermal fluxes. To evaluate this concern, a series of 1-D radial JPDR DORT cases was made using the same procedure as discussed above. These same 1-D cases were also modeled in XSDRN, which has a very efficient upscatter convergence algorithm. The tolerance for the XSDRN runs was less than 10^{-5} and convergence was achieved, in all cases, in less than 10 outers. With this tight convergence level, the XSDRN fluxes were considered to be the truth, and a direct comparison to the DORT-computed values were made to evaluate the accuracy of the DORT calculations. A series of flux ratio plots, with the XSDRN results as reference, are shown in Fig. 14. The fast and epithermal flux ratios are nearly unity which was the expected result -- illustrating that DORT and XSDRN give the same results for the same model. However, some differences, as large as $\pm 5\%$, were observed in the thermal fluxes. Thus, the unconverged DORT fluxes do introduce some uncertainty into the analyses performed here, but, as shown in Fig. 14, the effect is probably reasonably small. Even this small uncertainty is undesirable, and an enhanced iterative scheme in DORT would solve this problem as well as improve the overall computational efficiency of problems involving upscatter. The DORT improvements suggested here are certainly outside the scope of this project, but an improved

upscatter convergence scheme would definitely be a welcomed enhancement that could benefit many users.

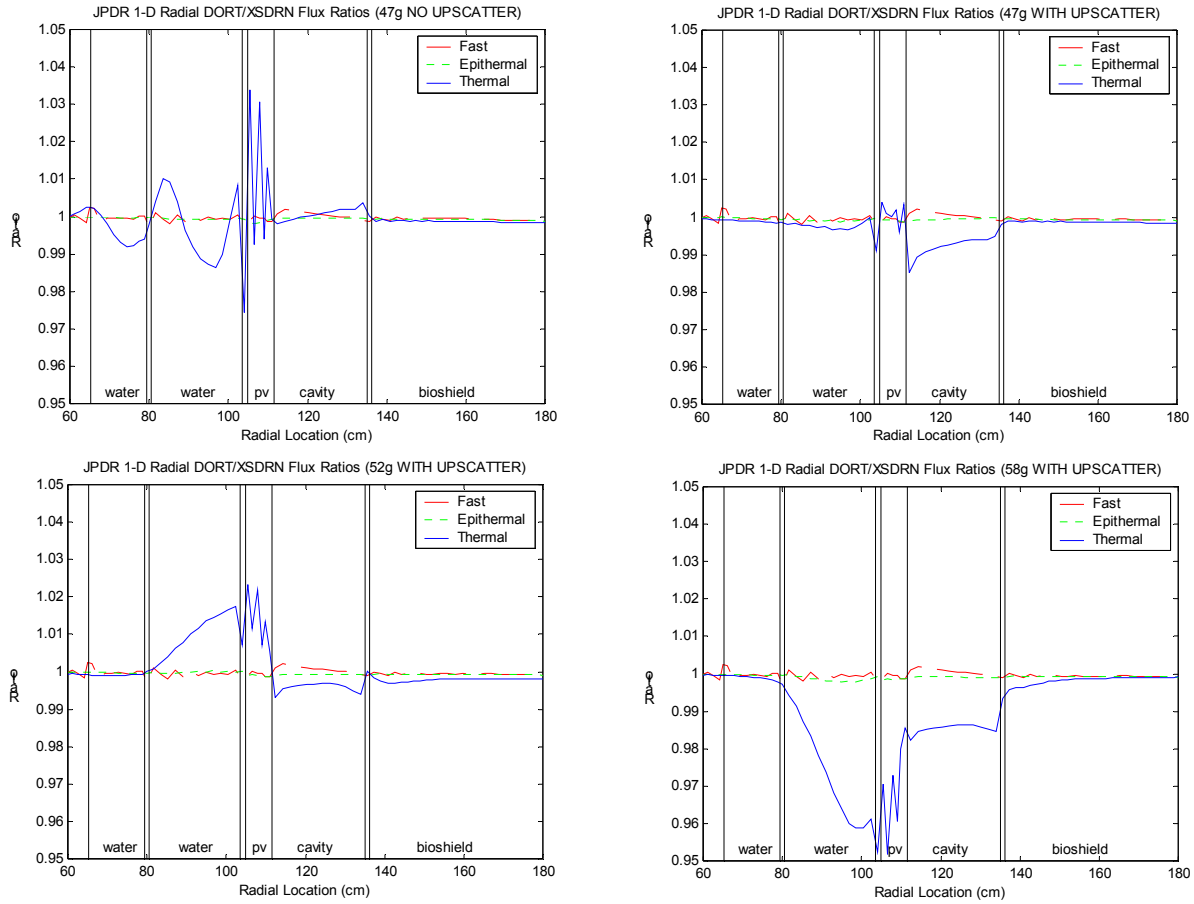

Fig. 14 Comparison of XSDRN and DORT calculations for the 1-D radial JPDR model.

Summary Conclusions/Recommendations

This study has shown that additional thermal energy resolution within the cross section library used for the transport calculations will produce a more reliable estimate of the thermal flux throughout the system. It has also shown that, with multiple thermal groups, the full upscatter treatment of the thermal scattering matrix is necessary. These findings are important in ex-core neutron activation computations because the thermal range is the most important region for most activation reactions.

Several BUGLE-like libraries, with the same energy structure as BUGLE-96 above 5 eV, but additional thermal energy groups, were generated and tested. A particular 58-group library with 16 thermal groups did especially well in comparison to a series of 199-group computations and it also performed well on the 2-D JPDR activation analysis benchmark. Thus, the 58-group library appears to be the best general-purpose transport library for use in generic ex-core neutron activation studies. Although the additional thermal groups with full upscatter capability results in a larger computational burden, the benefits of improved accuracy and reduced uncertainty seem to be well worth the additional effort. Improvements to the upscatter convergence

algorithm in the DORT code, in particular, would also simplify the overall solution process in many applications.

References

1. "SCALE 4.3 - Modular Code System for Performing Standardized Computer Analyses for Licensing Evaluation for Workstation and Personal Computers," Radiation Safety Information Computational Center,CCC-545 (1997). This package provides documentation for ORIGENS and most of the processing code used in this study (AJAX, BONAMI, NITAWL, MALOCS, XSDRN, etc.).
2. J. R. White and A. P. Fyfe, "UMass-Lowell Results for the JPDR Activation Analysis Benchmark," 1996 Topical Meeting on Radiation Protection and Shielding, No. Falmouth, Massachusetts (April 1996).
3. J. R. White, "Updated Results for the JPDR Activation Analysis Benchmark," 1998 ANS Radiation Protection and Shielding Topical Conference, Nashville, Tennessee (April 1998).
4. "DOORS3.1 - One, Two, and Three Dimensional Discrete Ordinates Neutron/Photon Transport Code System," Radiation Safety Information Computational Center, CCC-650 (1996).
5. "BUGLE-96 - Coupled 47 Neutron, 20 Gamma-Ray Cross Section Library Derived from ENDF/B-VI for LWR Shielding and Pressure Vessel Dosimetry Applications," Radiation Safety Information Computational Center, DLC-185 (1996).
6. I. Remec, "Two Benchmarks for Qualification of Pressure Vessel Fluence Calculational Methodology," 1998 ANS Radiation Protection and Shielding Topical Conference, Nashville, Tennessee (April 1998).
7. "VITAMIN-B6 - A Fine-Group Cross Section Library Based on ENDF/B-VI Release 3 for Radiation Transport Applications," Radiation Safety Information Computational Center, DLC-184 (1996).
8. T. Sukegawa, et. al., " Accuracy Verification for Calculation of Inventory in JPDR Due to Neutron Activation," International Atomic Energy Agency, INDC(JPN)-164 (1993).
9. Personal communication from L. M. Petrie, ORNL to J. R. White, UMass-Lowell (Feb. 1998).
10. N. Kocherov, "Benchmark on Radioactive Inventory Calculations for Fission Reactor Decommissioning," letter from IAEA to potential participants in benchmark exercise (1994).
11. B. L. Broadhead and R. L. Childs, "ORNL Contribution to the IAEA Benchmark Problem on Fission Reactor Decommissioning," 1996 Topical Meeting on Radiation Protection and Shielding, No. Falmouth, Massachusetts (April 1996).
12. S. J. Wall, et. al., "Current Status of UK Calculations for IAEA Decommissioning Benchmark (JPDR)," 1996 Topical Meeting on Radiation Protection and Shielding, No. Falmouth, Massachusetts (April 1996).
13. Personal communication from R. L. Childs, ORNL to J. R. White, UMass-Lowell (Aug. 1995).